Proceedings of the 9th International Conference of Control Systems, and Robotics (CDSR'22)
Niagara Falls, Canada – June 02-04, 2022
Paper No. 117
DOI: 10.11159/cdsr22.117

Nonlinear State Estimation and Control of an Organic Rankine Cycle

Daniel Sieben[1], Jeff Pieper[2]
[1]University of Calgary
Calgary, Alberta
dfsieben@ucalgary.ca; pieper@ucalgary.ca
[2]University of Calgary
Calgary, Alberta

Abstract - Waste heat recovery systems are designed to capture thermal energy from mechanical systems that would normally be transferred to their surroundings. Due to the stochastic nature of waste heat sources, control systems implemented to maintain process setpoints often have issues working with the apparent nonlinear, time-varying system. This work proposes using a Trans-critical Organic Rankine Cycle (TORC), where an organic working fluid is evaporated above its critical point, as a waste heat recovery system. The TORC system in this work is modelled as a 13-dimensional dynamic model with additive gaussian noise. An Extended Kalman Filter (EKF) is implemented to construct a full state estimate given a subset of noisy measurements which can be obtained with conventional sensors. Two different control systems are then implemented on this system. The first, a Cerebellar Model Articulation Control (CMAC), involves a proportional control output and a Neural Network learned output which satisfy the Lyapunov stability criterion. The second, an Iterative Linear Quadratic Regulator (ILQR), uses linearized points along a trajectory with a quadratic cost-function minimizing algorithm to choose control outputs. It was found that both the CMAC and ILQR can reliably track process setpoints and exhibit significantly less drift than linear control methods such as Proportional-Integral-Derivative Control.

***Keywords*:** Nonlinear Control, Nonlinear State Estimation, Organic Rankine Cycle, Optimal Control, Machine Learning

1. Introduction

Rankine Cycles are a common process for converting thermal energy from a heat source into mechanical energy which can then be further converted into electrical energy. Typically, a design goal for a Rankine Cycle is to maximize the thermal efficiency of the cycle, which is the ratio of power output from the cycle versus power input to the cycle, based around the expected temperature of the heat source. In this work a Rankine Cycle for capturing energy from low-quality heat sources, such as geothermal or industrial waste heat, is modelled and used in a dynamic simulation. This system, called a Transcritical Organic Rankine Cycle (TORC) originally modelled by Samiuddin et al. [1] shown in Fig. 1, utilizes three design components to improve the thermal efficiency of the cycle.

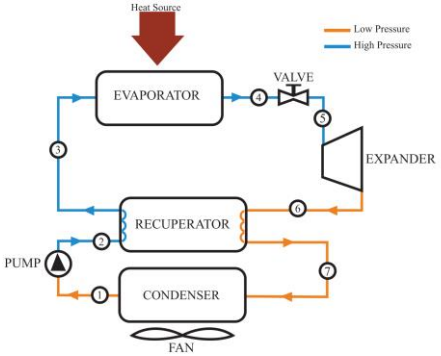

Fig. 1: Flow Diagram of the TORC System

The first design point is operating the evaporator in the supercritical-fluid phase of the working fluid, which allows for a larger enthalpy drop across the expander and thus a larger power output [2]. The second is using an organic working fluid instead of the more commonly used H2O as these typically have lower critical points that can be achieved with low-quality

heat sources and cheaper components. The last design point introduced in the model is the inclusion of a recuperator to transfer heat remaining in the working fluid back into itself before the evaporator.

The resulting dynamic model of the TORC system is a Nonlinear Time-Varying (NTV) system of equations represented in a 13-dimensional state. Since most common control systems in industry such as Proportional-Integral (PI) control are derived under the assumption that the system is Linear Time Invariant (LTI) it is likely they will not be able to reliably track process setpoints which are imposed on the system for performance and safety reasons. There have been proposed controls for similar Rankine Cycle systems in literature [1][2][3][4][5] which have included both Multiple-Input-Multiple-Output (MIMO) and Single-Input-Single-Output (SISO).

This work proposes using an Extended Kalman Filter (EKF) as a nonlinear state estimator to construct an optimal full state estimate out of a subset of noisy direct measurements of the state. Two control schemes are then implemented using the state estimate and compared to a typical PI control scheme. The first control method, an Iterative Linear Quadratic Regulator [6], is a locally optimal MIMO control method which iteratively converges a control policy using linearized points along a trajectory in order to minimize a quadratic cost function. The second control method, the Cerebellar Model Articulation Controller [7], uses a linear SISO control and a Neural Network learned output to determine control values.

2. Dynamic Modelling of the System

Modelling of the TORC is based on the work done by Samiuddin et al. [1] and involves three main dynamic components: the evaporator, the recuperator, and the condenser. The pump, valve, and expander components are modelled as static components. In each component the relevant fluid properties are determined by the pressure and enthalpy of the fluid. These are calculated in the simulation using the CoolProp library [8].

The complete TORC model, whose equations can be found in [1], has a 13-dimensional state

$$x = [P_{ev} \quad T_{out,ev} \quad T_{w,ev} \quad T_{out,h-rec} \quad T_{out,c-rec} \quad T_{w,rec} \quad L_1 \quad L_2 \quad P_c \quad T_{out,c} \quad T_{w1} \quad T_{w2} \quad T_{w3}]^T \tag{1}$$

three control variables are included in the system, given by

$$u = [X_{pump} \quad \mu_{valve} \quad N_{fan}]^T \tag{2}$$

and state transitions are computed in the form

$$\dot{x} = \Phi(x,u,\phi)^{-1}\Gamma(x,u,\phi) + W \sim Normal\left(0, \Sigma_{sys}\right) \tag{3}$$

Where Φ and Γ are nonlinear functions derived from the dynamic components mass and energy balance equations. W is a random variable representing a zero mean gaussian noise added to the system with covariance Σ_{sys} as a diagonal matrix arbitrarily chosen as 10% of the initial state.

Six measurements of state elements are made directly from the working fluid pressure and outlet temperature elements,

$$y = Cx + V \sim Normal(0, \Sigma_{meas}) \tag{4}$$

Where V is a random variable representing zero mean gaussian noise added to the system. Σ_{meas} is a diagonal matrix chosen with common standard deviations for temperature and pressure measurements.

For the purpose of demonstrating controls, 3 state references to converge the system to were arbitrarily chosen as

$$P_{ev} = 8\ MPa \tag{5}$$

$$T_{out,ev} = 630\ K \tag{6}$$

$$T_{w2} = 310\ K \tag{7}$$

3. State Estimation

Optimal state estimation of the TORC uses an Extended Kalman Filter (EKF) which solves the constrained optimization problem

$$J = E\left[\int_{t=t_1}^{t=T} \|x(\tau) - \hat{x}(\tau)\|\, d\tau\right] \tag{8}$$

$$\dot{x} = g(x,u) + W \sim Normal\left(0, \Sigma_{sys}\right) \tag{9}$$

$$y = h(x) + V \sim Normal(0, \Sigma_{meas}) \tag{10}$$

Where $x(t)$ and $\hat{x}(t)$ are the state and estimated state, respectively. $g(x,u)$ is the state transition function with additive noise according to a zero mean gaussian W with covariance Σ_{sys}. $h(x)$ is the state measurement function which is also subject to additive noise by zero mean gaussian V with covariance Σ_{meas}. In discrete form, the solution results in the following algorithm:

Given $y_1, \ldots, y_T$
Initialize $\hat{\mu}_0$, $\hat{\Sigma}_0$
For t = 1, …, T:

$$\bar{\mu}_t = g(\hat{\mu}_{t-1}, u_t) \tag{11}$$

$$G_t = \frac{d}{dx} g(\hat{\mu}_{t-1}, u_t) \tag{12}$$

$$\bar{\Sigma}_t = G_t \hat{\Sigma}_{t-1} G_t^T + \Sigma_{sys} \tag{13}$$

$$H_t = \frac{d}{dx} y(x) \tag{14}$$

$$K_t = \bar{\Sigma}_t H_t^T (H_t \bar{\Sigma}_t H_t^T + \Sigma_{meas})^{-1} \tag{15}$$

$$\hat{\mu}_t = \bar{\mu}_t + K_t\left(y_t - h(\bar{\mu}_t)\right) \tag{16}$$

$$\hat{\Sigma}_t = (I - K_t H_t)\bar{\Sigma}_t \tag{17}$$

Where $\hat{\mu}$ and $\hat{\Sigma}$ are the estimated mean and covariance of the system, respectively, and y_t are the actual system measurements at a given time. Eqs. (12) and (14) represent Jacobians of the state transition function $g(x,u)$ and the state measurement function $h(x)$. For the TORC, the state transition Jacobian is calculated numerically using two-point forward-difference differentiation while the measurement Jacobian is static due to the measurements of the system being direct.

4. Iterative Linear Quadratic Regulator

The ILQR [6] considers a cost function and system, respectively, of the form

$$J = \frac{1}{2}(x_T - r_T)^T Q_f (x_T - r_T) + \frac{1}{2}\sum_{t=0}^{T-1}((\mathrm{x_t} - r_t)^T Q(\mathrm{x_t} - r_t) + u_t^T R u_t) \tag{18}$$

$$x_{t+1} = g(x_t, u_t) \tag{19}$$

Where Q_f and Q are positive-semi-definite weighting matrices for the final state and the state over time, respectively. R is a positive-definite weighting matrix for the control effort. r_t is the state reference at any given time. By linearizing the system around an arbitrary nominal state x_t and control u_t a modified system can be considered

$$\delta x_{t+1} = A_t \delta x_t + B_t \delta u_t \tag{20}$$

In this linearization δx_t and δu_t are deviations from the nominal values. A_t and B_t are Jacobians of Eq. (19) with respect to x_t, u_t, calculated numerically. Solving the Linear Quadratic Regulator optimal control problem with this modified system results in the following algorithm:

Initialize x_t at its nominal points and δx_t as zero for all t = 0, …, T
Initialize u_t at its nominal points and δu_t as zero for all t = 0, …, T-1
While not converged:
For t = 0, …, T-1:

$$x_{t+1} = g(x_t, u_t) \tag{21}$$

$$A_t = \frac{d}{dx} g(x_t, u_t) \tag{22}$$

$$B_t = \frac{d}{du} g(x_t, u_t) \tag{23}$$

Initialize:

$$S_T = Q_f \tag{24}$$

$$v_T = Q_f(x_T - r_T) \tag{25}$$

For t = T-1, …, 0:

$$\theta_t = (B_t^T S_{t+1} B_t + R)^{-1} \tag{26}$$

$$K = \theta_t B_t^T S_{t+1} A_t \tag{27}$$

$$K_v = \theta_t B_t^T \tag{28}$$

$$K_u = \theta_t R \tag{29}$$

$$\delta u_t = -K\delta x_t - K_v v_{t+1} - K_u u_t \tag{30}$$

$$S_t = A_t^T S_{t+1}(A_t - B_t K) + Q \tag{31}$$

$$v_t = (A_t - B_t K)^T v_{t+1} - K^T R u_t + Q(x_t - r_t) \tag{32}$$

$$u_t = u_t + \delta u_t$$

For t = 0, …, T-1:

$$\delta x_{t+1} = A_t \delta x_t + B_t \delta u_t \tag{33}$$

For the TORC, Q is chosen as a modified identity matrix with the diagonal values corresponding to states given a reference changed to

$$Q_{i,i} = \frac{(r_i)^{-2}}{\sum_{j=0}^{n} (r_j)^{-2}} \tag{34}$$

Where n is the dimension of the state and r_i is the reference for a given state (or 0 if there is no reference). This is done to normalize the weightings of the states which are converging to a reference. The control weighting R is chosen as a normalized diagonal matrix of the maximum control limits. The TORC ILQR control implementation will use a 3-step-ahead prediction to plan control inputs. This is done to allow the control to compensate for changes resulting from the time-varying external heat source.

5. Cerebellar Model Articulation Controller

The CMAC follows the formulation from [1], where a Relative Gain Array analysis was performed and found the best SISO control pairings to be similar. The CMAC implementation in this work differs by having the input to the CMAC structure be a full state estimate from the EKF rather than the subset of noisy measurements. The structure of the CMAC is similar having the control output is determined by

$$u_i = u_{nom,i} + K_{p,i}e_i + \Gamma_i(q)\hat{w}_i \tag{35}$$

Where u_{nom} is a nominal control point chosen arbitrarily to introduce a bias, $K_p e$ is the proportional control output from from a normal linear controller, and $\Gamma(q)\hat{w}$ is the output of the neural network, with q being the chosen inputs of any dimension. The neural network structure quantizes the input q to determine active cells on each layer, as shown in Fig. 2.

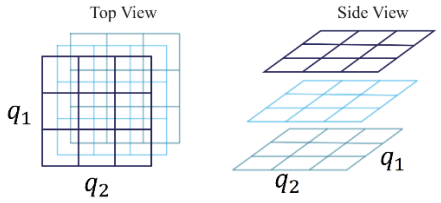

Fig. 2: CMAC Structure for Q=3, M=3, N=2

The CMAC is comprised of M layers, each with N inputs from the dimensionality of q, and Q quantizations. This results in MQ^N possible cells and corresponding weights. For a given input q only one cell per layer will be active by the definition of the activation function

$$\gamma(q) = \begin{cases} f(q), & if\ q\ is\ in\ cell\ i \\ 0, & otherwise \end{cases} \tag{36}$$

The vector $\Gamma(q)$ is then given by the activation of each cell per layer by their assigned function $f(q)$. For the TORC this is chosen as a spline function. Training of the neural network is done by a modified gradient descent algorithm [9] called e-modification, shown in Eq. (37)

$$\dot{\hat{w}} = \beta(\Gamma^T(q)e - \nu|e|\hat{w}) \tag{37}$$

Where β and ν are positive constants.

6. Simulation Results

For testing, the TORC simulation was subject to an external heat source modelled as a time-varying temperature and mass flow rate shown in Fig. 3.

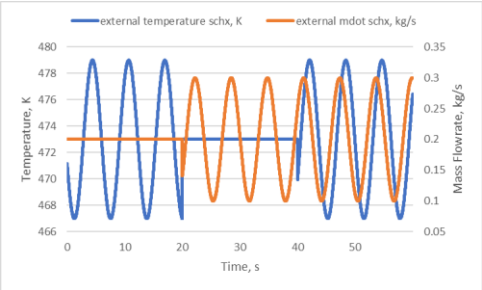

Fig. 3: External Heat Source Conditions

Sinusoids were chosen arbitrarily to produce a recognizable pattern in the control efforts and state as well as provide enough variation. As a comparison, the results of ILQR and CMAC control are plotted with similar results from a PI controller which was derived for the TORC system by Relay Autotuning [10].

6.1. State Estimation Results

For static control values and fluctuating external heat source conditions, the EKF was able to measure the state of TORC more accurately than the noisy direct measurements. The average error over the runtime was reduced by a factor approximately 47%, shown in Fig. 4.

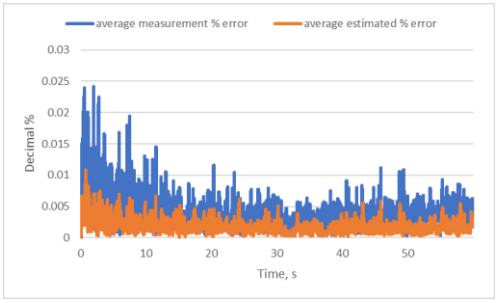

Fig. 4: Noisy Measurement vs. EKF Estimate Average Error

For states where no direct measurement is available the EKF performance was significantly worse, as shown in Fig. 5. The largest errors were found to be in the estimates of the condenser region lengths, shown in Fig. 6, indicating that their observability may be dependent on the state.

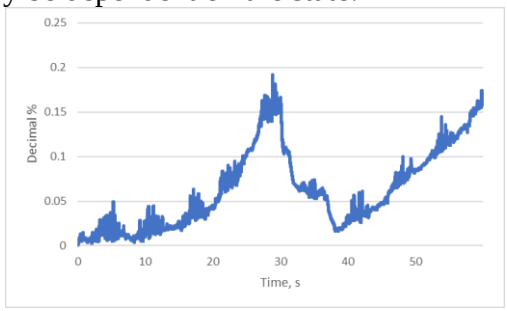

Fig. 5: EKF Average Error for Unmeasured State Elements

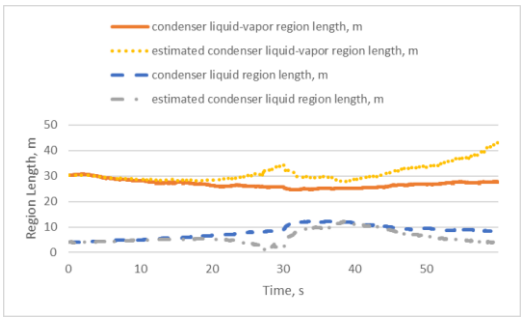

Fig. 6: EKF Estimates for Condenser Region Lengths

6.2. Controller Reference Tracking Results

Shown below in Fig. 7, Fig. 8, and Fig. 9 are the results of the reference tracking for the ILQR, CMAC, and PI controllers. While the ILQR controller typically converges the fastest, its performance is similar to the CMAC once the neural network has had a chance to converge. In comparison, the PI controller takes the longest to converge and is most susceptible to drastic changes due to the external heat source.

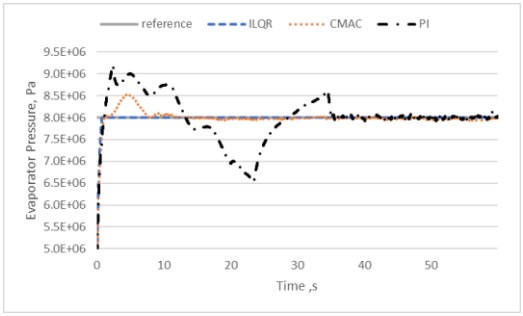

Fig. 7: Pev Reference Tracking Performance

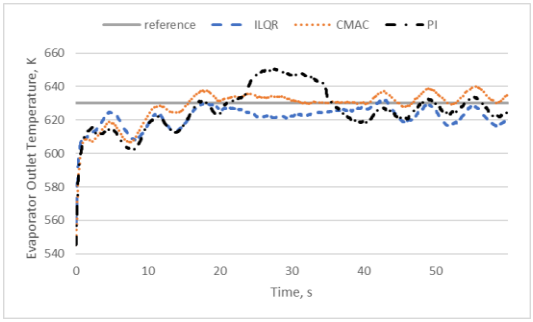

Fig. 8: Tout, ev Reference Tracking Performance

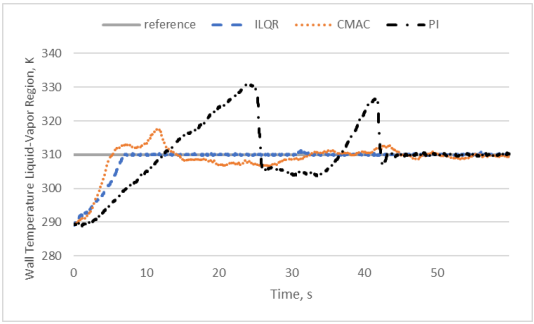

Fig. 9: T_{w2} Reference Tracking Performance

Table 1: Comparison of Control Methods Total Average Error over a Test Runtime

	PI	ILQR	CMAC
Total Average Error	2.698 %	0.654 %	0.899 %

7. Conclusion

In this work two control schemes were implemented on a TORC which show significant improvement in setpoint tracking over conventional PI controllers. The proposed EKF state estimator is shown to be effective in constructing a full state estimate given a subset of noisy measurements. The two control schemes, a MIMO ILQR optimal controller and a SISO CMAC neural network controller, are shown to have similar performance and are able to converge the NTV system to the reference much faster than a PI control scheme.

References

[1] J. Samiuddin, B. Badkoubeh-Hezaveh, M. Sadeghassadi, J. K. Pieper and C. J. B. Macnab, "Nonlinear adaptive control of a transcritical Organic Rankine Cycle," 2017 IEEE 26th International Symposium on Industrial Electronics (ISIE), pp. 513-519, 2017.

[2] S. Quoilin, R. Aumann, A. Grill, A. Schuster, V. Lemort, and H. Spliethoff, "Dynamic modeling and optimal control strategy of waste heat recovery organic rankine cycles," Applied Energy, vol. 88, no. 6, pp. 2183–2190, 2011.

[3] J. Zhang, W. Zhang, G. Hou, and F. Fang, "Dynamic modeling and multivariable control of organic rankine cycles in waste heat utilizing processes," Computers & Mathematics with Applications, vol. 64, no. 5, pp. 908–921, 2012.

[4] J. Zhang, Y. Zhou, Y. Li, G. Hou, and F. Fang, "Generalized predictive control applied in waste heat recovery power plants," Applied energy, vol. 102, pp. 320–326, 2013.

[5] J. Zhang, Y. Zhou, R. Wang, J. Xu, and F. Fang, "Modeling and constrained multivariable predictive control for orc (organic rankine cycle) based waste heat energy conversion systems," Energy, vol. 66, pp. 128–138, 2014.

[6] W. Li, E. Todorov, "Iterative Linear Quadratic Regulator Design for Nonlinear Biological Movement Systems", Proceedings of the First International Conference on Informatics in Control, Automation and Robotics, vol. 1, pp. 222-229, 2004.

[7] J. S. Albus, "A new approach to manipulator control: The cerebellar model articulation controller (cmac)," Journal of Dynamic Systems, Measurement, and Control, vol. 97, no. 3, pp. 220–227, 1975

[8] I. H. Bell, J. Wronski, S. Quoilin, V. Lemort, "Pure and Pseudo-pure Fluid Thermophysical Property Evaluation and the Open-Source Thermophysical Property Library CoolProp", Industrial & Engineering Chemistry Research, vol. 53, no. 6, 2014, pp. 2498-2508.

[9] K. Narendra and A. Annaswamy, "A new adaptive law for robust adaptation without persistent excitation," IEEE Transactions on Automatic Control, vol. 32, no. 2, pp. 134–145, Feb. 1987.

[10] P. D. Rohitha, S. Senadheera and J. K. Pieper, "Fully automated PID and lead/lag compensator design tool for industrial use," Proceedings of 2005 IEEE Conference on Control Applications, pp. 1009-1014, 2005.